CrossMark

J. Fluid Mech. (2005), *vol.* 522, *pp.* 63–89. © 2005 Cambridge University Press
DOI: 10.1017/S0022112004001363 Printed in the United Kingdom

Rotating gravity currents. Part 2. Potential vorticity theory

By J. R. MARTIN[1]†, D. A. SMEED[2] AND G. F. LANE-SERFF[3]

[1]School of Ocean & Earth Science, Southampton Oceanography Centre, University of Southampton, Waterfront Campus, European Way, Southampton SO14 3ZH, UK

[2]Southampton Oceanography Centre, University of Southampton, Waterfront Campus, European Way, Southampton SO14 3ZH, UK

[3]Manchester Centre for Civil and Construction Engineering, UMIST, PO Box 88, Manchester M60 1QD, UK
g.f.lane-serff@umist.ac.uk

(Received 17 January 2003 and in revised form 21 July 2004)

An extension to the energy-conserving theory of gravity currents in rectangular rotating channels is presented, in which an upstream potential vorticity boundary condition in the current is applied. It is assumed that the fluid is inviscid; that the Boussinesq approximation applies; that the fundamental properties of momentum, energy, volume flux and potential vorticity are conserved between upstream and downstream locations; and that the flow is dissipationless. The upstream potential vorticity in the current is set through the introduction of a new parameter δ, that defines the ratio of the reference depth of the current to the ambient fluid. Flow types are established as a function δ and the rotation rate, and a fourth flow geometry is identified in addition to the three previously identified for rotating gravity currents. Detailed solutions are obtained for three cases $\delta = 0.5$, 1.0 and 1.5, where $\delta < 1$ is relevant to currents originating from a shallow source and $\delta > 1$ to currents where the source region is deeper than the downstream depth, for example where a deep ocean flow encounters a plateau. The governing equations and solutions for each case are derived, quantifying the flow in terms of the depth, width and front speed. Cross-stream velocity profiles are provided for both the ambient fluid and the current. These predict the evolution of a complex circulation within the current as the rotation rate is varied. The ambient fluid exhibits similar trends to those predicted by the energy-conserving theory, with the Froude number tending to $\sqrt{2}$ at the right-hand wall at high rotation rates. The introduction of the potential vorticity boundary condition into the energy-conserving theory does not appear to have a substantial effect on the main flow parameters (such as current speed and width); however it does provide an insight into the complex dynamics of the flow within the current.

1. Introduction

This is the second of two papers examining the dynamics of gravity currents in rotating fluids. Hacker (1996) developed a model in which the current was considered to be a cavity around which the ambient fluid flowed, and the ambient fluid was assumed to

† Present affiliation: Southampton University Hospitals NHS Trust, Mail Point 79, Southampton General Hospital, Tremona Road, Southampton SO16 6YD, UK; jrmartin2@ntlworld.com

https://doi.org/10.1017/S0022112004001363 Published online by Cambridge University Press

conserve energy and potential vorticity. Following the approach of Benjamin (1968) for non-rotating flows, Martin & Lane-Serff (2004) extended Hacker's theory to allow for energy loss in the ambient fluid. The model developed in that paper, which forms the first part of this study and hereafter is referred to as Part 1, does not consider flow within the current.

In the present paper we develop a theory which allows for flow within the gravity current (though it does not allow for energy loss). There are two reasons for extending the model in this way: first, to obtain a description of the expected flow within the current; and, second, to examine whether the flow within the current has a significant effect on the propagation of the current.

In considering the limitations of his energy-conserving theory Hacker noted that the potential vorticity distribution in the current was not prescribed but was instead determined by the solution for a particular level of rotation, W. He conjectured that an upstream potential vorticity boundary condition could be included if the constraints of conservation of volume flux and potential vorticity within the current are met. These can be expressed as

$$\int_S u_c(y)\,\mathrm{d}S = 0, \tag{1.1}$$

$$\int_S u_c(y) q_c(y)\,\mathrm{d}S = 0, \tag{1.2}$$

where u_c and q_c are the alongstream velocity and the potential vorticity of the current, and the surface S is a cross-section through the current in the (y, z)-plane.

For lock-release experiments in which fluid is released from an initially stationary and uniform-depth reservoir, the potential vorticity of the current is uniform, and we will consider this case in the following analysis. The ambient and gravity current fluids are coupled by Magule's balance at the interface, and so allowing a non-zero velocity in the current modifies the ambient flow too. The cross-stream flow structure of two-layer flows with uniform potential vorticity has been derived by authors studying geostrophic adjustment (e.g. van Heijst 1985; Casandy 1971, 1978; Stommel & Veronis 1980; Ou 1983; and Hsueh & Cushman-Roisin 1983). The flow is the solution of a second-order differential equation. In the problem of geostrophic adjustment the two constants in the solution are determined from the conservation of mass and of angular momentum. In this paper we derive alternative conditions appropriate for a steady-state gravity current. In § 2 this method is applied to give the general solution for the depth of the interface. Governing equations are then derived for each of the flow geometries. The numerical solutions are presented in § 3 and finally in § 4 the results are discussed.

2. The model

2.1. *Outline*

The derivation is divided into three stages. In stage 1, conservation of potential vorticity for the ambient fluid and the current is considered. The equations are non-dimensionalized and a new parameter, the ratio $\delta = H_c/H$, is introduced, where H_c is the depth of the current fluid in an upstream stationary reservoir. Thus we assume that the potential vorticity in the current is uniform, and is effectively described by the value of f/H_c. Next, the Margules equation is used to determine the relationship between the slope of the interface between the two layers and the velocity jump across

https://doi.org/10.1017/S0022112004001363 Published online by Cambridge University Press

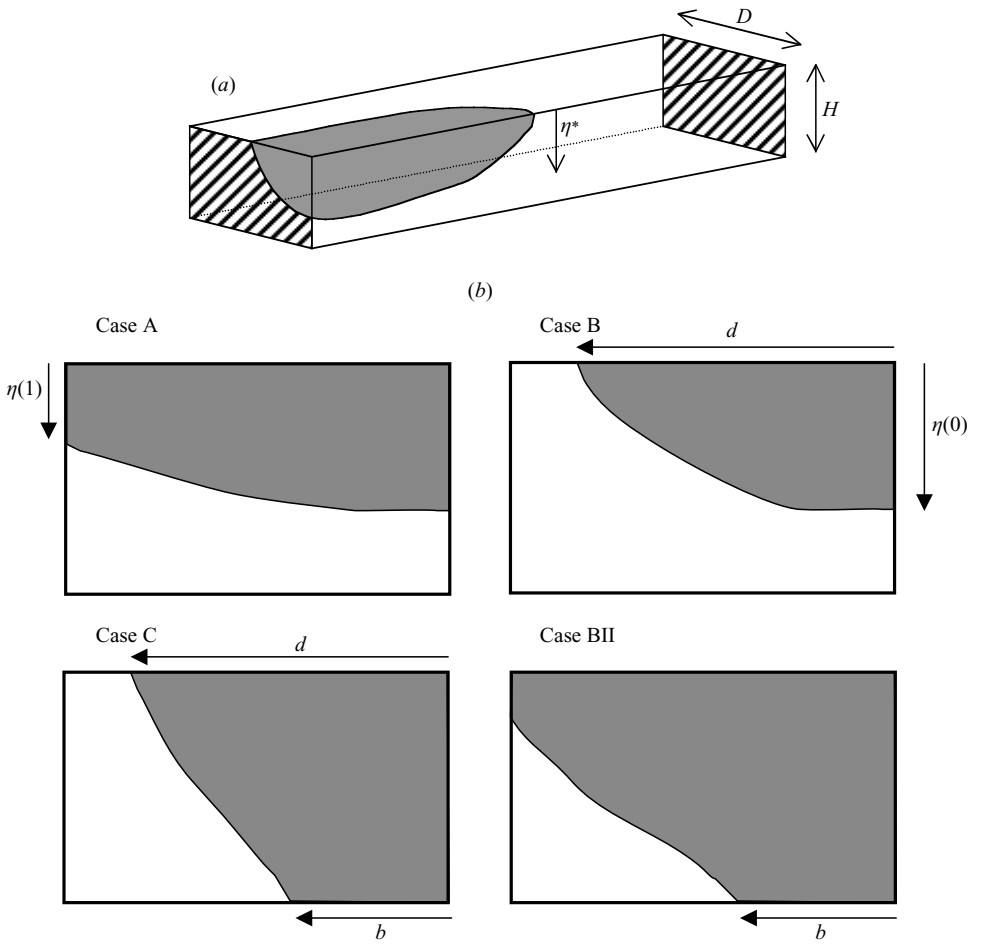


FIGURE 1. (*a*) Sketch of a rotating gravity current in a channel of width D and height H, with the (dimensional) interface depth η^*. (*b*) Sketches of the four flow geometries (in non-dimensional form), which depend on which boundaries the interface intersects.

the interface. From these, general solutions defining the structure of the flow in terms of five parameters are obtained: $u_c(0)$, the downstream velocity of the current at the right-hand wall; $u_D(0)$, the downstream velocity of the ambient fluid at the right-hand wall; η_0, the depth of the current at the right-hand wall; c, the speed of translation of the reference frame; and p_0, the upstream pressure in the ambient fluid.

In stage 2, conservation of the fundamental properties energy, mass and momentum between up- and downstream cross-sections are considered. Finally, in stage 3 these conditions are applied to each of the four flow geometries illustrated in figure 1 (there is an extra geometry compared with those described in Part 1, discussed further in § 2.4). This results in a complex set of simultaneous equations for each case. Note that the assumptions made in the earlier energy-conserving theory of rotating gravity currents are still applicable with the exception that a recirculating flow is allowed within the current. The adjustment of the current from the initial source conditions is assumed to be inviscid, with no energy loss in the current, hence potential vorticity is conserved.

https://doi.org/10.1017/S0022112004001363 Published online by Cambridge University Press

Basic scales

The main features of a rotating gravity current in a rectangular channel are illustrated in figure 1. Most of the parameters and variables are similar to those in Part 1. Thus the parameters and variables in the model are defined and non-dimensionalized as follows. The dimensional variables are marked with an asterisk. Vectors are in bold type. The subscripts c and a refer to the current and ambient fluid respectively, with U the upstream and D the downstream locations. The subscript 0 specifies a variable measured at the right-hand wall, which is therefore a constant. Where a symbol appears only once, it is defined in the text.

The reduced gravity is given by $g' = g\Delta\rho/\rho_a$ where $\Delta\rho = \rho_a - \rho_c$, the channel width is D, the channel depth H, and the Coriolis parameter f. We define a Rossby radius in terms of the total channel depth $R = f/(g'H)^{1/2}$. The aspect ratio of the channel is denoted by $\lambda_H = H/D$, and we also define a density ratio $\rho = \rho_c^*/\rho_a^* = 1 - \Delta\rho^*/\rho_a^*$. For Boussinesq flow we can take $\rho = 1$. We non-dimensionalize distances and speeds as follows:

$$\left.\begin{array}{ll} \text{horizontal lengths} & x = x^*/D, \quad y = y^*/D, \\ \text{vertical lengths} & z = z^*/H, \quad \eta = \eta^*/H, \\ \text{velocities} & \boldsymbol{u} = \boldsymbol{u}^*/(g'H)^{1/2}, \\ \text{velocity of the leading edge} & c = c^*/(g'H)^{1/2}, \\ \text{pressure} & p = (p^* - \rho_a^* g z^*)/(\rho_a^* g' H). \end{array}\right\} \tag{2.1}$$

Note that in addition to scaling the pressure term we also remove a hydrostatic component. An important parameter is the strength of the rotation; this is characterized by the ratio of the width of the channel to the Rossby radius of deformation: $W = fD/(g'H)^{1/2}$.

There is an extra dimensional parameter compared with Part 1: H_c, the reference depth that specifies the potential vorticity for the current. This leads to a corresponding non-dimensional parameter,

$$\delta = H_c/H. \tag{2.2}$$

As in Part 1, the solution is independent of the aspect ratio (λ) and the density ratio (ρ). In the present model, the solution is dependent on the strength of rotation W and the potential vorticity ratio δ. Below we show that an alternative description of the strength of rotation is useful, represented by the parameter W' (see § 2.2).

2.2. *Stage 1 – Downstream flow structure*

Conservation of potential vorticity

As in Part 1, the ambient fluid upstream of the current head is assumed to be motionless, so that in the frame of reference moving with the current head the upstream ambient flow is uniform with velocity -c along the channel. In this subsection we consider a section far downstream where the flow is parallel to the channel so that

$$\boldsymbol{u}_c = (u_c(y, z), 0, 0) \tag{2.3}$$

and

$$\boldsymbol{u}_a = (u_a(y, z), 0, 0). \tag{2.4}$$

The subscript a, refers to the ambient fluid, which can be further divided into the ambient fluid up and downstream, by the subscripts U and D respectively. The

https://doi.org/10.1017/S0022112004001363 Published online by Cambridge University Press

subscript c refers to the current. Since the flow in the current is recirculating u_c may take either sign, while the ambient flow is always negative.

Conservation of potential vorticity in the current and the ambient fluid imply that

$$\frac{f-(\mathrm{d}u_c/\mathrm{d}y)}{\eta}=\frac{f}{H_c} \tag{2.5}$$

and

$$\frac{f-(\mathrm{d}u_D/\mathrm{d}y)}{H-\eta}=\frac{f}{H}. \tag{2.6}$$

Non-dimensionalizing (2.5) and (2.6) gives, for the current

$$\frac{\mathrm{d}u_c}{\mathrm{d}y}=W(1-\eta/\delta), \tag{2.7}$$

and for the ambient fluid

$$\frac{\mathrm{d}u_D}{\mathrm{d}y}=W\eta. \tag{2.8}$$

Geostrophic equations and Margules relationship

To remove the hydrostatic pressure variation with depth in the current, p_c may be written as

$$p_c=P_c+(z-1). \tag{2.9}$$

The non-dimensionalized momentum equations for the current (Part 1: (2.8)) and the ambient fluid (Part 1: (2.9)) are still applicable. Applying the Boussinesq approximation ($\rho=1$) and (2.9) the geostrophic relationship for the current becomes

$$\frac{\mathrm{d}p_c}{\mathrm{d}y}=\frac{\mathrm{d}P_c}{\mathrm{d}y}=-W(u_c+c). \tag{2.10}$$

For the ambient fluid the new sign convention (2.3) implies

$$\frac{\mathrm{d}p_D}{\mathrm{d}y}=-W(u_D+c). \tag{2.11}$$

Since the pressure is continuous at the interface between the two fluids where $z=1-\eta$, this implies that

$$p_D=P_c-\eta. \tag{2.12}$$

Differentiating (2.12) and substituting (2.10) and (2.11) gives the Margules (1906) relationship, where the slope of the interface between the two fluids is given by the difference in velocity across the interface

$$u_c-u_D=-W^{-1}\mathrm{d}\eta/\mathrm{d}y. \tag{2.13}$$

Flow structure equations

The general solution for $\eta(y)$ is derived by first differentiating (2.13) with respect to y, and substituting (2.7) and (2.8) to give

$$-W^2=\mathrm{d}^2\eta/\mathrm{d}y^2-W'^2\eta, \tag{2.14}$$

where

$$W'^2=W^2(1+\delta)/\delta=\frac{f^2D^2(H+H_c)}{g'HH_c}.$$

https://doi.org/10.1017/S0022112004001363 Published online by Cambridge University Press

Note that when we consider the flow in the current the lengthscale for the cross-stream structure is changed from $1/W$ in Part 1 to $1/W'$.

Equation (2.14) is only valid for $0 < \eta < 1$; however the interface may intersect the surface or the bottom of the channel. We define the location at which the interface intersects the bottom as $y = b$, with $b = 0$ if the interface does not intersect the bottom (i.e. $\eta < 1$ at $y = 0$). Similarly we define $y = d$ as the location where the interface intersects the upper surface, with $d = 1$ if the interface does not intersect the surface (i.e. $\eta > 0$ at $y = 1$). The general solution of (2.14) in $b < y <$d is

$$\eta(y) = \delta/(1+\delta) + A\cosh W'(y-b) + B\sinh W'(y-b), \tag{2.15}$$

where A and B are constants of integration which are solved subsequently. The general solutions for $u_c(y)$ and $u_D(y)$ are obtained by substituting (2.15) into (2.7) and (2.8) respectively to give

$$u_c(y) = E + W(\delta/(1+\delta))y - (W/\delta W')[A\sinh W'(y-b) + B\cosh W'(y-b)] \tag{2.16}$$

and

$$u_D(y) = F + W(\delta/(1+\delta))y + (W/W')[A\sinh W'(y-b) + B\cosh W'(y-b)]. \tag{2.17}$$

Subtracting (2.17) from (2.16) and equating with (2.13) shows that the two constants in (2.16) and (2.17) are equivalent, i.e. $E = F$. Returning to the constants A and B in the above equations these are obtained by considering the solutions of (2.5) at $y = b$. Hence, (2.15) becomes

$$A = \eta(b) - (\delta/(1+\delta)). \tag{2.18}$$

The constant B is obtained by subtracting the solution at $y = b$ of (2.17) from the solution at $y = b$ of (2.16) which gives

$$B = -W/W'(u_c(b) - u_D(b)). \tag{2.19}$$

Substituting the expressions for the constants A (2.18) and B (2.19) into the general solutions (2.16) and (2.17) and evaluating them at $y = b$ enables the remaining constant F to be determined, where

$$\begin{aligned} E = F &= u_c(b) - (W^2/\delta W'^2)(u_c(b) - u_D(b)) = u_D(b) + (W^2/W'^2)(u_c(b) - u_D(b)) \\ &= u_c(b) - (1+\delta)^{-1}(u_c(b) - u_D(b)). \end{aligned} \tag{2.20}$$

Substituting the expressions for the coefficients A and B into (2.15) enables the general solution for $\eta(y)$ to be written as

$$\begin{aligned} \eta(y) = \delta/(1+\delta) &+ (\eta(b) - \delta/(1+\delta))\cosh W'(y-b) \\ &+ ((-W/W')(u_c(b) - u_D(b)))\sinh W'(y-b). \end{aligned} \tag{2.21}$$

Thus the structure of the flow is defined in terms of its depth and the respective velocities of the current and the ambient fluid at $y = b$. However, we also need to consider what happens when the interface intersects the upper or lower boundaries. Setting $\eta = 0$ in (2.15) we find that the interface intersects the upper boundary at $y = d$, given by

$$\eta(d) = 0 = \delta/(1+\delta) + A\cosh W'(d-b) + B\sinh W'(d-b) \tag{2.22}$$

where A and B are the constants defined in (2.18) and (2.19). The value of b (where it is greater than zero) has to be found indirectly through a Bernoulli equation (see below).

https://doi.org/10.1017/S0022112004001363 Published online by Cambridge University Press

The flows in the current for $0 < y < b$ and in the ambient for $d < y < 1$ (i.e. where the relevant fluid layer occupies the full depth of the channel) are found by applying the conservation of potential vorticity (2.5 and 2.6, respectively) and continuity at $y = b$ and $y = d$. Thus if $d < 1$, then u_D is constant for $y > d$, i.e. $u_D(y) = u_D(d)$ for $d < y < 1$, and if $b > 0$, then

$$u_c(y) = u_c(b) + W[(\delta - 1)/\delta](y - b) \quad \text{for} \quad 0 < y < b. \tag{2.23}$$

Pressure equations

The pressure in each layer can be evaluated by integrating the geostrophic relations (2.10) and (2.11) making use of the full expressions for the velocities (and noting that $(\delta/(1+\delta)) = W^2/W'^2$) to give

$$\begin{aligned} P_c = k + 1 - Wcy - W \Bigg[& \left(u_c(0) - \left(\frac{W^2}{\delta W'^2} \right) (u_c(0) - u_D(0)) \right) y + \tfrac{1}{2} W \left(\frac{\delta}{(1+\delta)} \right) y^2 \\ & - \left(\frac{W}{\delta W'^2} \right) \left(\left(\eta_0 - \frac{\delta}{(1+\delta)} \right) \cosh W'(y-b) \right. \\ & \left. + \left(\left(\frac{-W}{W'} \right) (u_c(0) - u_D(0)) \right) \sinh W'(y-b) \right) \Bigg] \end{aligned} \tag{2.24}$$

and

$$\begin{aligned} p_D = k - Wcy - W \Bigg[& \left(u_c(0) - \left(\frac{W^2}{\delta W'^2} \right) (u_c(0) - u_D(0)) \right) y + \tfrac{1}{2} W \left(\frac{\delta}{(1+\delta)} \right) y^2 \\ & - \left(\frac{W}{\delta W'^2} \right) \left(\left(\eta_0 - \frac{\delta}{(1+\delta)} \right) \cosh W'(y-b) \right. \\ & \left. + \left(\left(\frac{-W}{W'} \right) (u_c(0) - u_D(0)) \right) \sinh W'(y-b) \right) \Bigg] + 1 - \eta. \end{aligned} \tag{2.25}$$

Note that there is an additional constant k. Thus the complete flow is described by five parameters: $u_c(0)$, $u_D(0)$, η_0 (or b if $\eta_0 = 1$), k and c. To determine the values of these constants we will apply conservation of energy and momentum. These constraints will be discussed in the next section.

2.3. *Stage 2 – Conservation of the fundamental properties*

Conservation of energy

In Part 1, for the case in which the flow in the current $u_c = 0$, two of the three equations required to determine the flow were derived from consideration of the conservation of energy in the ambient fluid. It can be shown that this applies equally to the current fluid, and we will use it to derive two further equations necessary to complete the problem, i.e. we will use the Bernoulli equations for the current and the ambient

$$\left.\begin{aligned} B_c &= \tfrac{1}{2}|\boldsymbol{u}_c|^2 + P_c(y) + Wcy = \text{constant along streamlines,} \\ B_a &= \tfrac{1}{2}|\boldsymbol{u}_a|^2 + P_a(y) + Wcy = \text{constant along streamlines.} \end{aligned}\right\} \tag{2.26}$$

Applying the Bernoulli equation for the current along a streamline connecting the forward stagnation point (0, 0, 1) to a point on the right-hand boundary downstream in the current gives

$$B_c(0) = 0 = \tfrac{1}{2}u_c(0)^2 + P_c(0) \tag{2.27}$$

https://doi.org/10.1017/S0022112004001363 Published online by Cambridge University Press

(defining the pressure at the stagnation point to be zero). Hence, the downstream pressure in the current is quantified as

$$-\tfrac{1}{2}u_c(0)^2 = P_c(0). \tag{2.28}$$

This then determines the value of k (see Appendix A), giving the first in our set of equations. To obtain the value of $B_c(d)$, first (2.26) is differentiated and use is made of the geostrophic and the potential vorticity equations (2.10) and (2.7) respectively to give

$$\frac{\mathrm{d}B_c}{\mathrm{d}y} = \frac{-W\eta u_c}{\delta}.$$

Integrating the above expression and making use of condition (1.1), that states that there is no flux of fluid into or out of the current, gives

$$B_c(d) - B_c(0) = -\frac{W}{\delta}\int_0^d u_c(y)\eta(y)\,\mathrm{d}y = -\frac{W}{\delta}[Q_c(y)]_0^d = 0. \tag{2.29}$$

According to (2.28) $B_c(0) = 0$, which implies that $B_c(d) = 0$, therefore (2.29) becomes

$$B_c(d) = \tfrac{1}{2}u_c(d)^2 + P_c(d) + Wcd = 0. \tag{2.30}$$

Alternatively (2.30) could have been derived by considering a streamline originating at the forward stagnation point and extending along the outer edge of the current. Thus we see that the conservation of volume does not provide any additional information over that which can be obtained from the Bernoulli equation.

Hence, we have derived two Bernoulli equations (2.27) and (2.30) for the current. Two equations for the ambient can be derived by following a similar analysis to that in Part 1, giving

$$B_D(b) = 0 = \tfrac{1}{2}u_D^2(b) + p_D(b) + Wcb, \tag{2.31}$$

and

$$B_D(1) = Wc = \tfrac{1}{2}u_D^2(1) + p_D(1) + Wc. \tag{2.32}$$

In cases A and B (see figure 1) where $b = 0$, $B_D(0)$ becomes

$$B_D(0) = \tfrac{1}{2}u_D(0)^2 + p_D(0).$$

Applying (2.12) at $b = 0$ and making use of (2.28) gives

$$\eta_0 = \tfrac{1}{2}u_D(0)^2 - \tfrac{1}{2}u_c(0)^2. \tag{2.33}$$

Next, integrating the relationship obtained in the derivation of (2.28), for case C where $y \in [0, b]$ yields

$$B_c(b) - B_c(0) = -\frac{W}{\delta}\int_0^b u_c(y)\eta(y)\,\mathrm{d}y. \tag{2.34}$$

Applying $B_c(0) = 0$ (2.27) and (2.7), (2.34) becomes

$$B_c(b) = \frac{u_c^2(b)}{2(1-\delta)} - \frac{u_c^2(0)}{2(1-\delta)}. \tag{2.35}$$

Equating (2.35) with (2.26) applied at $y = b$ gives

$$-\tfrac{1}{2}u_c^2(b)\frac{\delta}{1-\delta} + P_c(b) + Wcb + \frac{1}{2(1-\delta)}u_c^2(0) = 0. \tag{2.36}$$

https://doi.org/10.1017/S0022112004001363 Published online by Cambridge University Press

Substituting (2.12) into (2.31) and equating with (2.36) gives

$$-\tfrac{1}{2}u_c^2(b)\frac{\delta}{1-\delta}+\frac{1}{2(1-\delta)}u_c^2(0)=\tfrac{1}{2}u_D^2(b)-\eta(b). \tag{2.37}$$

The integral of (2.7) for $y\in[0,b]$ is

$$u_c(b)-u_c(0)=Wb\,((\delta-1)/\delta), \tag{2.38}$$

which is substituted into (2.37) to give

$$\tfrac{1}{2}u_D^2(b)=\tfrac{1}{2}u_c^2(b)+\frac{Wb}{\delta}u_c(b)+W^2b^2\frac{1-\delta}{2\delta^2}+\eta(b). \tag{2.39}$$

The relationship (2.39) defines $u_D(b)$ in terms of $u_c(b)$ and b, which can be further defined in terms of η_0, $u_c(0)$ and $u_D(0)$ for $y=0$. Equation (2.39) forms the second equation in the set of five necessary to complete the solution.

Next we derive an equation for the current speed, c, by considering Bernoulli equations for the downstream flow in the ambient fluid. The derivation is similar to that in Part 1 and is omitted here, but the full derivation is given in Appendix A. The result is

$$c=W^{-1}\left[\tfrac{1}{2}u_D(1)^2-\tfrac{1}{2}u_c(d)^2+WU_D(d-1)-\eta(d)\right] \tag{2.40}$$

Equation (2.40) is the third general equation required to close the problem. Note that when $u_c=0$ is substituted into (2.40) expressions are obtained for each of the cases that are equivalent to those derived in the energy-conserving theory with simple flow.

Now the pressure difference across the current is considered. Again the details are omitted here and the full derivation is given in Appendix A; the result is

$$\begin{aligned}\tfrac{1}{2}\left(u_c^2(d)-u_c^2(b)\right)&=\frac{(d-b)}{(1+\delta)}(W(u_D(b)+\delta u_c(b)))\\&\quad+\frac{1}{1+\delta}\left(\eta(b)-\eta(d)+\tfrac{1}{2}W^2\delta(d-b)^2\right)+\frac{Wb}{\delta}u_c(b)+W^2b^2\frac{1-\delta}{2\delta^2}.\end{aligned} \tag{2.41}$$

This is the fourth in our set of four general equations derived from conservation of energy.

Conservation of momentum

Conservation of momentum is evaluated as in § 2.2 of Part 1. The momentum equations (Part 1: (2.8)) and (Part 1: (2.9)) are integrated over the rectangular volume between the up- and downstream cross-sections. However, in this model the velocity of the current is not assumed to equal zero and therefore must be included. The divergence theorem is again used to express the advective and pressure terms as surface integrals (note that at rigid boundaries $\boldsymbol{u}\cdot\boldsymbol{n}=0$

$$\begin{aligned}\int_{A_U+A_a+A_c}\boldsymbol{u}(\boldsymbol{u}\cdot\boldsymbol{n})\,\mathrm{d}S+\int_{\partial V_a+\partial V_c}p\boldsymbol{n}\,\mathrm{d}S&=-\int_{V_c+V_c}Wkx\boldsymbol{u}\,\mathrm{d}V\\&\quad-Wcj\int_{V_a+V_c}\mathrm{d}V+\boldsymbol{k}\int_{V_c}\mathrm{d}V.\end{aligned} \tag{2.42}$$

The volume V is bounded by ∂V with subscripts a and c referring to the ambient fluid and current respectively. The up- and downstream faces of ∂V are A_U and A_D, where A_D is composed of A_c and A_a. Considering the different components of (2.42), one finds that the total Coriolis force acting in the i-direction is equivalent to the

https://doi.org/10.1017/S0022112004001363 Published online by Cambridge University Press

sum of the net fluxes of the momentum plus the pressure force acting on the wall in the i-direction, where

$$\int_{A_U} \left(u_u^2 + p_u\right) \mathrm{d}A - \int_{A_a} \left(u_D^2 + p_D\right) \mathrm{d}A - \int_{A_c} \left(u_c^2 + p_c\right) \mathrm{d}A = W \int_{V_a+V_c} v \, \mathrm{d}V. \quad (2.43)$$

Note that the expression for conservation of momentum derived in Part 1 has been altered to include the non-zero velocity of the current. There now also exists an across-stream velocity, v_c, in the current. This induces a Coriolis force directed upstream (for positive v_c) with respect to the current, which acts to retard the current.

The j-component expresses the balance between the net pressure force on the sidewalls, and the sum of the Coriolis force and the body force of translation. The k-component represents the balance between the net pressure force on the top and bottom walls, and the buoyancy force acting on the current. The j- and k-components are not used in the analysis: the remaining unknowns are determined from the i-component.

Using the fact that $u_U = -c$ and the substitution for the upstream pressure (Part 1: A 1), expression (2.43), becomes

$$\tfrac{1}{2}c^2 = \int_{A_c} \left(u_c^2 + p_c\right) \mathrm{d}A + \int_{A_a} \left(u_D^2 + p_D\right) \mathrm{d}A + W \int_{V_c} v_c \, \mathrm{d}V + W \int_{V_a} v_D \, \mathrm{d}V. \quad (2.44)$$

The solution of (2.44) is quite complex. The solution method is broken down into a number of steps summarized below, with the full details given in Appendix A.

Step 1: The integrals associated with first the current, and secondly the ambient fluid, are reduced to single integrals.
Step 2: The terms used previously in Part 1 in deriving conservation of energy with simple flow are then considered.
Step 3: The remaining terms for the current, which result from relaxing the zero velocity assumption, are considered next.
Step 4: The terms derived in steps 2 and 3 are combined to produce a simplified version of (2.44), which contains two single integrals.
Step 5: These are evaluated, where possible by substituting exact differentials and making use of the Bernoulli equations, to produce the general solution for the momentum integral.

After this manipulation (details in Appendix A), equation (2.44) can be reduced to

$$\tfrac{1}{2}c^2 = \int_b^d \tfrac{1}{2}(-u_c(u_D + \delta u_c)) \, \mathrm{d}y + \frac{1}{W}\left[\frac{\delta^2}{6(1-\delta)} u_c^3\right]_0^b + \left[\frac{\delta}{6W} u_c^3\right]_0^d + \frac{1}{W}\left[\frac{1}{6}u_D^3 - \tfrac{1}{2}u_D\eta - u_D B_D(y)\right]_b^d + \tfrac{1}{2}U_D^2(1-d) - \tfrac{1}{2}b. \quad (2.45)$$

To evaluate the integral in (2.45) it is necessary to substitute the expressions for the flow structure and then integrate (see Appendix A).

Summary of the general form of the governing equations

The problem is now fully specified. There are five general equations: the momentum integral (2.45) and four Bernoulli equations (2.28), (2.39), (2.40) and (2.41). For each case the relevant boundary conditions b and d are found from equations (2.22) and (2.24) and applied to these general equations. Next the flow structure equations (2.21), (2.25) and (2.26) are substituted enabling the resulting equations to be expressed in

https://doi.org/10.1017/S0022112004001363 Published online by Cambridge University Press

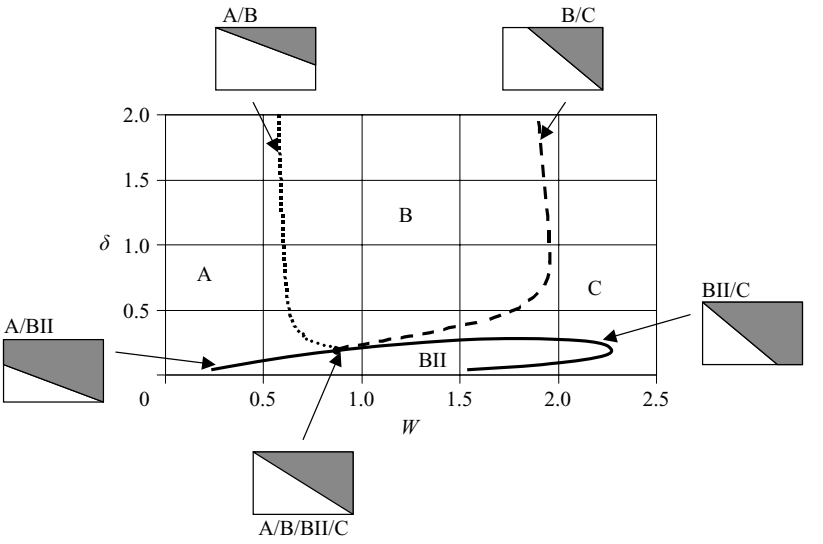


FIGURE 2. Regime diagram showing the different flow types (found numerically) as functions of the rotation strength W and PV ratio δ. The sketches are schematic representations of the flows at the boundaries for the four main flow types (at these boundaries the interface intersects a corner).

terms of the four variables, $u_c(\mathrm{b})$, $u_D(\mathrm{b})$, $\eta(\mathrm{b})$ and c, which are thus functions of the parameters W and δ. The four simultaneous equations can then be solved to find the flow for any values of the parameters.

The flow geometries

The general form of the governing equations can now be applied to each of the flow geometries, which are dependent upon the strength of the rotation (as sketched in figure 1). Due to the complexity of the governing equations and the absence of a simple relationship between $u_c(b)$ and $u_D(b)$, a numerical method is required to solve the equations for each case. The detailed equations for each case, together with some notes on their numerical solution, are given in Appendix B.

The numerical method was first applied to the three flow geometries identified in Part 1. These are case A, weakly rotating flow with the interface intersecting both sidewalls and thus $b=0$, $d=1$; case B, flows of moderate rotation with the interface outcropping on the surface and thus $b=0$, $d<1$; and case C, strongly rotating flows with the interface outcropping on the lower and upper surface, and thus $0<b<d<1$. From the numerical calculations it became clear that a fourth flow geometry was possible, occurring at small values of δ and moderate values of W. This was labelled case BII, and has the interface intersecting the left sidewall (looking downstream with respect to the current) and the lower boundary, and thus has $b>0$ and $d=1$.

3. Results

The parameter range for which solutions were obtained is illustrated in figure 2, showing the different flow geometries as functions of W and δ. Since the solutions are forced to be energy-conserving, the predicted current depths are all of the order of half the channel depth (recall that the non-rotating energy-conserving solution has a current depth of exactly half the channel depth). As δ represents the upstream reservoir

https://doi.org/10.1017/S0022112004001363 Published online by Cambridge University Press

depth of the fluid in the gravity current, values of δ greater than approximately 0.5 represent flows where the depth of the fluid has decreased between the reservoir and the current, leading to anticyclonic relative vorticity in the current. Conversely, values of δ less than approximately 0.5 represent flows where the current has increased in depth leading to cyclonic vorticity in the current. It is hard to envisage how a real flow might increase in depth, so that the flows for small δ may not be physically realizable. However, there may be other mechanisms which give rise to gravity currents with cyclonic relative vorticity, so we discuss the behaviour at small δ first.

Small δ

The flow geometry BII is only found for values of $\delta < 0.27$ and $W < 2.3$, and is presumably associated with strongly cyclonic recirculating flow within the current. At certain fixed values of δ it is possible to move through all the flow geometries as W increases, in the order A, B, C, BII, C. This can be accomplished by both the typical interface slope and the lower boundary intercept b increasing monotonically with rotation rate W. The boundaries in parameter space between the cases all have the interface intercepting the channel boundary at the top-left or bottom-right corner (looking downstream with respect to the current). As the interface moves away from the corner the flow becomes one of the four main cases. There is a point in parameter space (at approximately $\delta = 0.19$, $W = 0.9$) which corresponds to the interface intercepting the boundary at both corners. The boundaries on figure 2 were determined by solving the flow at specific values of W and δ, and the positions are estimated to be accurate to ± 0.005 in δ and ± 0.05 in W, though we have not attempted to formally determine the behaviour as $\delta \to 0$.

Large δ

At larger values of δ, an increase in rotation rate W results in a progression through the flow geometries found in Part 1, with only a weak dependence of the transition values on the value of δ. Detailed solutions have been obtained for three cases where $\delta = 0.5$, 1.0 and 1.5. In this theory the principle variables are a function of two parameters, W and δ. Figure 3 shows the solutions for the front speed c as W is increased, for each of the three values of δ.

One can see that the value of δ appears to have no significant effect upon the front speed, with all of the solutions for c plotting close to the energy-conserving solution of Hacker. In case A (weak rotation, $0 \leqslant W \leqslant 0.67$), the current fills the full width of the channel and the front speed is seen to increase approximately linearly. In case B, (moderate rotation, $0.67 \leqslant W \leqslant 1.8$) the current outcrops on the free surface and the increase in c becomes more gradual. Finally, in case C (strong rotation, $1.8 \leqslant W \leqslant 3.0$) the current fills the full depth of the channel as c tends towards 1 at high rotation rates.

An important aspect of this theory is that it provides solutions for the velocity profile within the current, $u_c(y)$, which was assumed to be zero in the earlier theories. To illustrate the solutions, velocity profiles for the current and the ambient fluid are provided for each value of δ. The outer edge of the current is marked by $+$ and labelled with its respective value. Positive velocity is towards the nose of the current whilst negative velocity is away from the nose. The interface profiles are also included. The method used to contour the solutions is Delaunay Triangulation and the data set contains more than 1500 data points. Figure 4 contains contour plots of the across-stream current velocity, $u_c(y)$ for $\delta = 0.5$, 1.0 and 1.5.

For the case of $\delta = 0.5$ the circulation within the current shows marked differences to that seen for the other values of δ. At weak rotation rates the direction of flow

https://doi.org/10.1017/S0022112004001363 Published online by Cambridge University Press

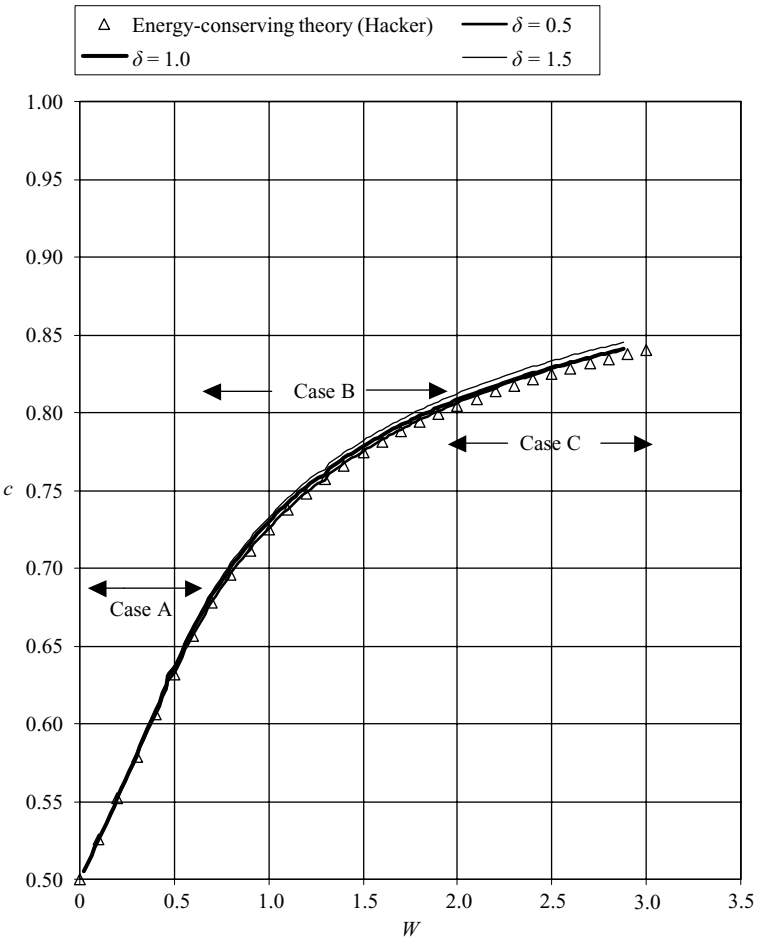


FIGURE 3. Comparison of front speed, c, versus rotation rate, W, for each of the values of δ and the energy-conserving theory of Hacker.

in the current at the right-hand wall is negative. Midway across the stream the direction of the flow switches to positive, therefore an anticyclonic circulation has developed. As the level of rotation is increased a more complex flow develops, with a cyclonic flow next to the right-hand wall and an anticyclonic flow at the outer edge of the current. The boundary between the two flows occurs at $\eta(y) = 0.5$, i.e. $\delta = \eta(y)$. This can be explained by a simple physical argument in that the fluid has undergone vortex stretching at the right-hand wall whilst at the outer edge of the current the fluid has experienced vortex compression. The stretching of the vortex lines requires that the water column has to take on additional cyclonic relative vorticity to conserve its potential vorticity, whilst the compression requires additional anticyclonic relative vorticity. Mathematically this behaviour is described by the potential vorticity equation (2.7). When $\delta = \eta(y)$, as is the case when $\delta = 0.5$ and $\eta(y) = 0.5$, then $\mathrm{d}u_c/\mathrm{d}y = 0$. The second derivative of (2.7) is positive; therefore when $\delta = \eta(y) = 0.5$ there is a minimum value for u_c. This can clearly be seen by comparing figures 4(a) and 6(a).

On comparing the velocity $u_c(y)$ at $y = d$ for each value of δ, the velocity is found to increase at the outer edge of the current as δ is increased. However at the right-hand

https://doi.org/10.1017/S0022112004001363 Published online by Cambridge University Press

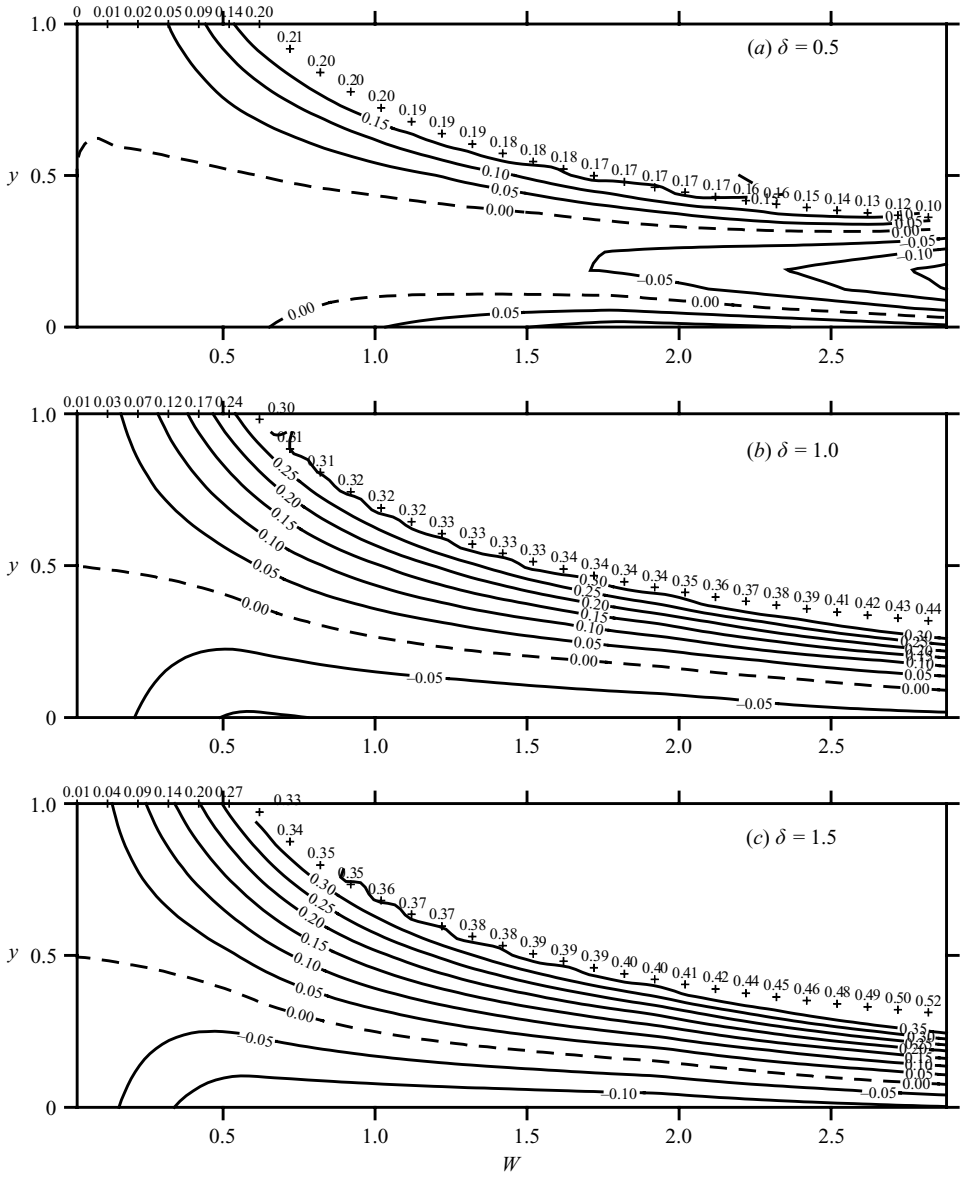


FIGURE 4. Velocity of the current (which varies across the width of the current) $u_c(y)$ for $\delta = 0.5$, 1.0 and 1.5, as a function of the rotation rate. The width of the current for each rotation rate is denoted by crosses, with the value of the velocity at the current edge marked.

wall $u_c(0)$ decreases, hence there is an increase in the strength of the circulation as δ becomes greater.

Figure 5 illustrates the flow in the ambient fluid, which is always in the negative direction as one would expect. There is little variation in $u_D(y)$ as δ is varied and the across-stream profiles are similar to that observed for the energy-conserving theory of Hacker. At weak rotation rates u_D is seen to increase in magnitude at the right-hand wall. This is because the pressure at $y = 0$ is not a function of W and is instead influenced by the increasing depth of the interface and $u_c(0)$. At high rotation

https://doi.org/10.1017/S0022112004001363 Published online by Cambridge University Press

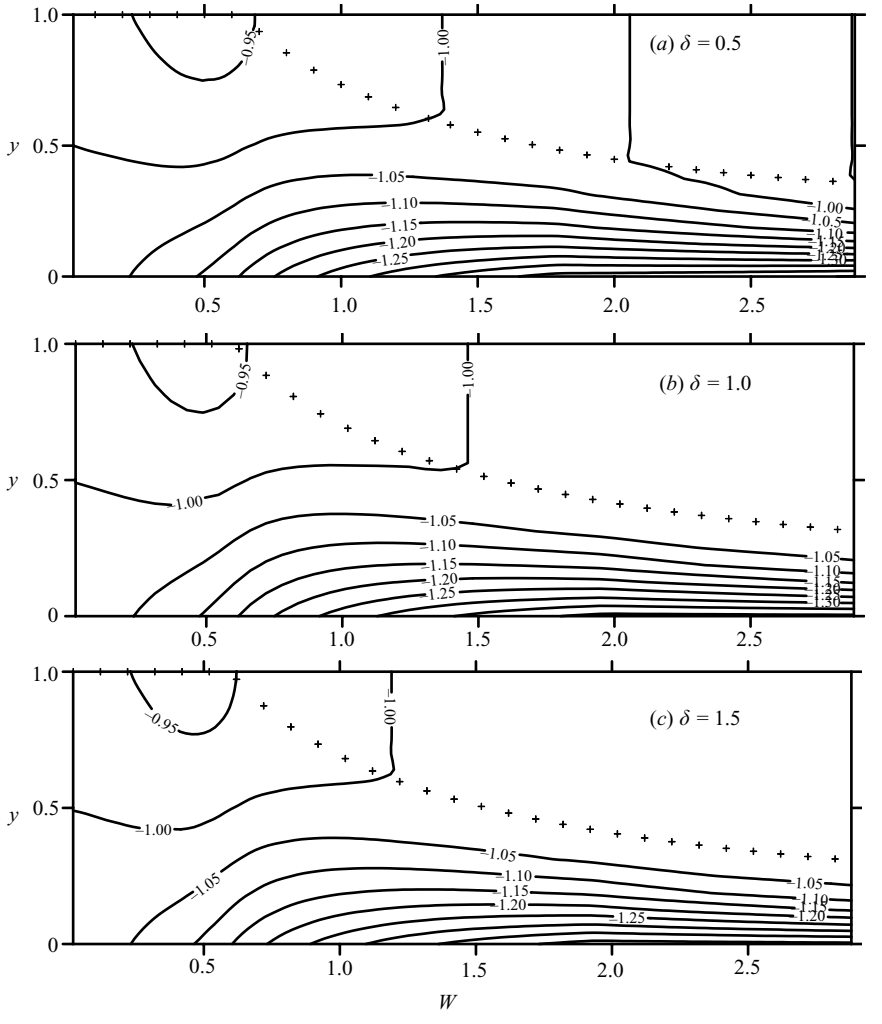


FIGURE 5. Velocity of the ambient fluid $u_D(y)$ for $\delta = 0.5$, 1.0 and 1.5, as a function of the rotation rate.

rates $u_D(0)$ tends to $-2^{1/2}$. At the left-hand wall the pressure is a balance between the hydrostatic and geostrophic pressure gradients. At weak rotation rates the hydrostatic pressure is dominant and since the depth of the interface is decreasing at the left-hand wall this results in an increase in pressure, which is associated with a deceleration of the flow. As W increases further the influence of the geostrophic pressure gradient is seen and in the free stream the ambient velocity is seen to increase, tending to -1.

The depth profiles for each of the values of δ are shown in figure 6. These profiles are very similar, with the only discernible difference being the slight increase in the width of the current for $\delta = 0.5$.

4. Summary and discussion

To summarize, the effects of introducing a potential vorticity boundary condition in the source region are first, that the circulation within the current has little effect upon the front speed, c. Hacker explained the variation in front speed with rotation

https://doi.org/10.1017/S0022112004001363 Published online by Cambridge University Press

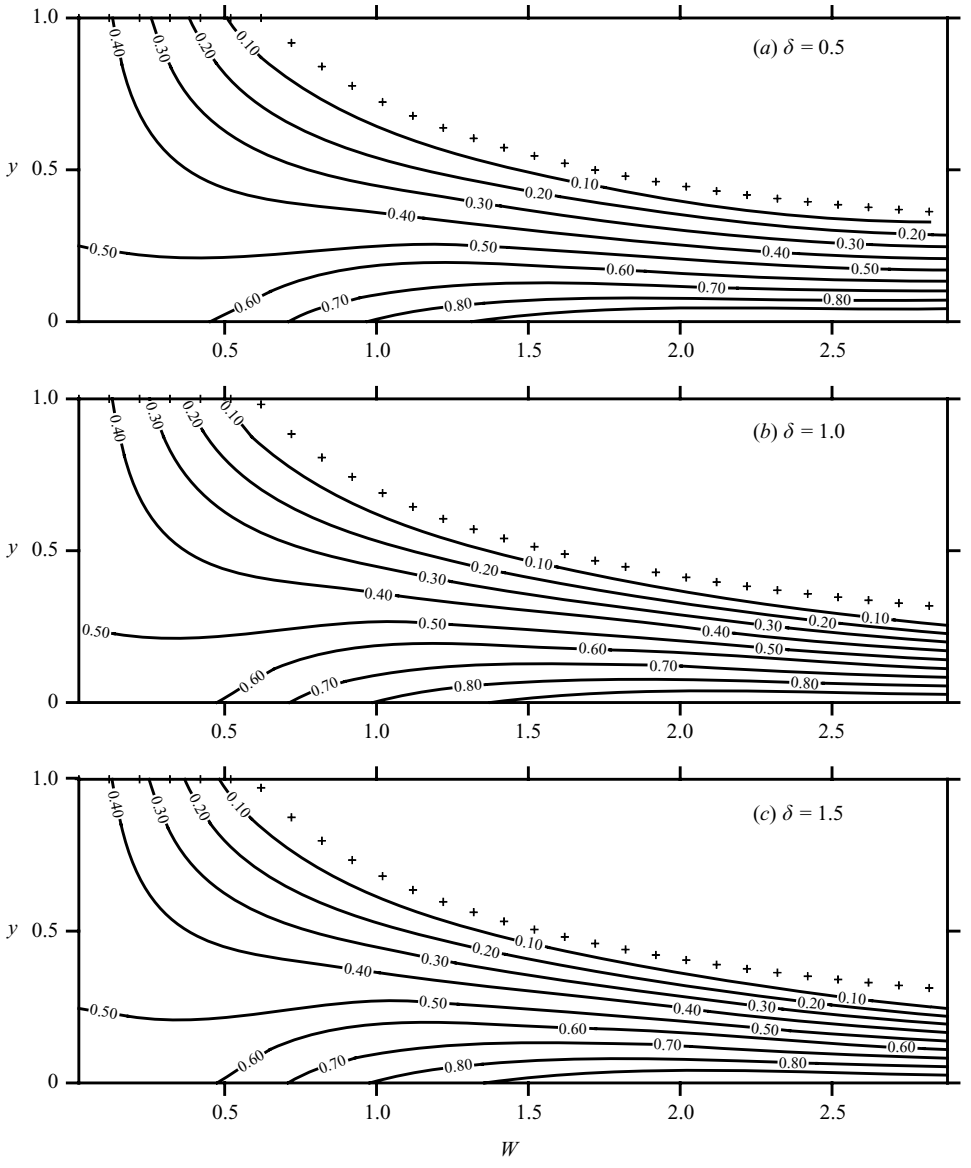


FIGURE 6. Across-stream depth of the current $\eta(y)$ for $\delta = 0.5$, 1.0 and 1.5, as a function of the rotation rate. The edge of the current (where $\eta(y) = 0$) is marked by crosses.

by a simple argument based on continuity of volume flux. This same argument can be used to explain why the front speed was not significantly altered by the inclusion of potential vorticity (PV) upstream, since it is dependent upon the downstream cross-sectional area of the ambient fluid. In the PV theory the depth profile and the ambient fluid velocity remained approximately the same as that observed in the energy-conserving theory of Hacker; therefore the volume flux across a downstream cross section must be similar. This would demand the same speed of the oncoming flow as in the energy-conserving theory of Hacker to ensure conservation of volume flux.

https://doi.org/10.1017/S0022112004001363 Published online by Cambridge University Press

Secondly, a complex circulation was seen to develop within the current for $\delta = 0.5$, with cyclonic circulation nearest the right-hand wall and anticyclonic at the outer edge of the current. These converged at $\eta(y) = 0.5$. This was explained using a simple physical argument based on whether the flow experienced vortex compression or stretching. For the cases $\delta = 1.0$ and $\delta = 1.5$ the current experienced an anticyclonic circulation, whilst the velocity of the ambient fluid showed similar trends to those of the energy-conserving solutions of Hacker, i.e. with the Froude number tending to $\sqrt{2}$ at the right-hand wall and 1 in the free stream at high rotation rates.

Thirdly, the numerical results indicate that a fourth flow geometry is possible for small values of δ and, although it is hard to envisage how this flow might arise from simple flow out of a reservoir, such solutions (with strong cyclonic vorticity) might have practical applications.

The theory we have developed here to include uniform PV in the source has provided an insight into the circulation which develops within the current. However, varying the pre-set PV in the source region does not appear to have a substantial effect upon the front speed or the other parameters which describe the flow. Therefore, one may conclude that the theory of Hacker (with no pre-set PV in the source region) provides an adequate description of the main features of the energy-conserving flow. Similarly, this suggests that the energy dissipation theory presented in Part 1 – which also assumes no shear within the current – is likely to give similar results for flow speed and width as a more complicated theory which might (in principle) be developed to include PV effects (in addition to energy dissipation).

Much of this work was carried out at the School of Ocean and Earth Science, University of Southampton, where J.R.M. was supported by a PhD studentship from the Natural Environment Research Council (UK) and G.F.L.S. was supported by a University Research Fellowship from the Royal Society, London. J.R.M. was granted sabbatical leave to prepare this paper by Southampton University Hospitals NHS Trust. The authors would like to thank Professor Steve Thorpe for useful discussions and advice.

Appendix A. Derivation of the energy and momentum equations

Much of the detailed derivation of the equations needed to solve the dissipationless and potential vorticity conserving flows has been omitted from the main text and is given in this appendix.

A.1. *Energy equations*

In order to define the Bernoulli equations for the downstream flow in the ambient fluid, for $y \in [b, d]$ and $y \in [d, 1]$, in terms of the principal variables, expressions for the pressure $p_D(y)$ are required. First, the constant of integration k in the pressure equations (2.24) and (2.25) is found: (2.24) is evaluated at $y = 0$ and the substitution (2.27) is applied to give

$$k = -\tfrac{1}{2}u_c(0)^2 - 1 - (W^2/\delta W'^2)(\eta_0 - (W^2/W'^2)). \tag{A 1}$$

Hence (2.24) becomes, for $y \in [b, d]$,

$$\begin{aligned} P_c(y) = {} & -\tfrac{1}{2}u_c(0)^2 - (W^2/\delta W'^2)\eta_0 + (W^4/\delta W'^4) - Wcy \\ & - W[u_c(0) - (W^2/\delta W'^2)(u_c(0) - u_D(0))]y - \left(\tfrac{1}{2}W^4/W'^2\right)y^2 \\ & + (W^2/\delta W'^2)(\eta(y) - W^2/W'^2). \end{aligned} \tag{A 2}$$

https://doi.org/10.1017/S0022112004001363 Published online by Cambridge University Press

For the ambient fluid (2.25) for $y \in [b, d]$ becomes

$$\begin{aligned} p_D(y) = &-\tfrac{1}{2}u_c(0)^2 - (W^2/\delta W'^2)\eta_0 + (W^4/\delta W'^4) - Wcy \\ &- W[u_c(0) - (W^2/\delta W'^2)(u_c(0) - u_D(0))]y - \left(\tfrac{1}{2}W^4/W'^2\right)y^2 \\ &+ (W^2/\delta W'^2)(\eta(y) - (W^2/W'^2)) - \eta. \end{aligned} \tag{A 3}$$

In the free stream around the current $\eta(d) = 0$, hence the pressure at $y \in [d, 1]$ is obtained by first substituting (2.21) applied at $y = d$ into (A 3) to give the boundary condition

$$\begin{aligned} p_D(d) = &-\tfrac{1}{2}u_c(0)^2 - (W^2/\delta W'^2)\eta_0 - Wcd \\ &- W[u_c(0) - (W^2/\delta W'^2)(u_c(0) - u_D(0))]\, d - \left(\tfrac{1}{2}W^4/W'^2\right) d^2. \end{aligned} \tag{A 4}$$

An expression for the pressure in the free stream is obtained by integrating the geostrophic equation (2.11), which gives

$$p_D(y) = -WU_D y - Wcy + H.$$

Applying the above expression at $y = d$ and equating with (A 4) enables the integration constant H to be solved; hence

$y \in [d, 1]$:

$$\begin{aligned} p_D(y) = &\, WU_D(d - y) - Wcy - \tfrac{1}{2}u_c(0)^2 - (W^2/\delta W'^2)\eta_0 \\ &- W[u_D(0) - (W^2/W'^2)(u_c(0) - u_D(0))]\, d - \left(\tfrac{1}{2}W^4/W'^2\right) d^2. \end{aligned} \tag{A 5}$$

Applying (A 5) at $y = 1$ gives

$$\begin{aligned} p_D(1) = &\, WU_D(d - 1) - Wc - \tfrac{1}{2}u_c(0)^2 - (W^2/\delta W'^2)\eta_0 \\ &- W[u_D(0) - (W^2/W'^2)(u_c(0) - u_D(0))]\, d - \left(\tfrac{1}{2}W^4/W'^2\right) d^2. \end{aligned} \tag{A 6}$$

It is now possible to write the expressions for conservation of energy in the ambient fluid in terms of the principal variables and parameters defining the flow structure; therefore substituting (A 3) into a Bernoulli equation gives

$y \in [b, d]$:

$$\begin{aligned} B_D(y) = WcY(y) = &\tfrac{1}{2}u_D(y)^2 - \tfrac{1}{2}u_c(0)^2 - (W^2/\delta W'^2)\eta_0 + (W^4/\delta W'^4) \\ &- W\left[u_D(0) - (W^2/W'^2)(u_c(0) - u_D(0))y - \tfrac{1}{2}W^4/W'^2\right]y^2 \\ &+ (W^2/\delta W'^2)((\eta_0 - (W^2/W'^2))\cosh W'y \\ &+ ((-W/W')(u_c(0) - u_D(0))\sinh W'y) - \eta(y). \end{aligned} \tag{A 7}$$

Substituting (A 5) into a Bernoulli equation gives

$y \in [d, 1]$:

$$\begin{aligned} B_D(y) = WcY(y) = &\tfrac{1}{2}U_D^2 + WU_D(d - y) - \tfrac{1}{2}u_c(0)^2 - (W^2/\delta W'^2)\eta_0 \\ &- W\left[u_D(0) - (W^2/W'^2)(u_c(0) - u_D(0))\, d - \tfrac{1}{2}W^4/W'^2\right] d^2. \end{aligned} \tag{A 8}$$

Applying (A 8) at $y = d$ and $y = 1$ the following relationship is obtained:

$y \in [d, 1]$:

$$B_D(d) = B_D(1) + WU_D(1 - d). \tag{A 9}$$

https://doi.org/10.1017/S0022112004001363 Published online by Cambridge University Press

At $y=d$, $\eta=0$ which according to (2.12) implies that $P_c=p_D$, hence

$$B_D(d) = \tfrac{1}{2}U_D^2 + P_c(d) + Wcd$$
$$= \tfrac{1}{2}\big(U_D^2 - u_c(d)^2\big). \tag{A 10}$$

It is now possible to complete the expressions for conservation of energy in the ambient fluid by first substituting (A 3) applied at $y=b$ into (2.31), which becomes

$$B_D(b) = 0 = \tfrac{1}{2}u_D(b)^2 - \tfrac{1}{2}u_c(0)^2 - (W^2/\delta W'^2)\eta_0$$
$$- W(u_c(0) - (W^2/W'^2)(u_c(0) - u_D(0)))b - \big(\tfrac{1}{2}W^4/W'^2\big)b^2 - \delta/(1+\delta). \tag{A 11}$$

Secondly $B_D(1)$ is calculated where $Y(1)=1$. An equation which may be applied to all the flow geometries is obtained by combining the expressions for $B_D(1)$ for case A with that for cases B and C. The equation for case A is found by substituting (A 3) applied at $y=1$ into (2.32). For cases B and C (A 6) is substituted into (2.32). The resulting equation is

$$B_D(1) = Wc = \tfrac{1}{2}u_D(1)^2 + WU_D(d-1) - \tfrac{1}{2}u_c(0)^2 - (W^2/\delta W'^2)\eta_0$$
$$- W(u_D(0) - (W^2/W'^2)(u_c(0) - u_D(0)))d - \big(\tfrac{1}{2}W^4/W'^2\big)d^2$$
$$+ (W^2/\delta W'^2)\eta(d) - \eta(d). \tag{A 12}$$

According to (2.30)

$$-\tfrac{1}{2}u_c(d)^2 = P_c(d) + Wcd. \tag{A 13}$$

Substituting (2.12) into (A 13) and noting (2.20), enables (A 12) to be simplified. It is now possible to define c in terms of the principal variables,

$$c = W^{-1}\big[\tfrac{1}{2}u_D(1)^2 - \tfrac{1}{2}u_c(d)^2 + WU_D(d-1) - \eta(d)\big]. \tag{A 14}$$

Equation (A 14), which is (2.40) in the main text, is the third equation required to close the problem.

The conditions for $y\in[b,d]$ are now considered. Substituting (2.14) into the potential vorticity equation (2.8) enables it to be integrated between the limits $y\in[b,y]$. The substitution (2.13) is then introduced and the expression is rearranged to become

$$u_D(y) + \delta u_c(y) - W\delta y = u_D(b) + \delta u_c(b) - W\delta b, \tag{A 15}$$

using

$$u_c = \frac{1}{1+\delta}((u_c - u_D) + (u_D + \delta u_c)). \tag{A 16}$$

The differential (2.13) replaces the first term in the brackets. To obtain a substitution for the second term the following integral is considered and equated with (A 15) to give

$$\delta\int_b^y \frac{\mathrm{d}u_c}{\mathrm{d}y}\mathrm{d}y = \delta(u_c(y) - u_c(b))$$
$$= u_D(b) - u_D(y) + W\delta(y-b).$$

The integral above enables a substitution for the second term in (A 16) to be obtained,

$$u_c(y) = \frac{1}{1+\delta}\left(-\frac{1}{W}\frac{\mathrm{d}\eta}{\mathrm{d}y} + W\delta(y-b) + (u_D(b) + \delta u_c(b))\right). \tag{A 17}$$

https://doi.org/10.1017/S0022112004001363 Published online by Cambridge University Press

Integrating (A 17) between the limits $y \in [b, d]$ gives

$$\int_b^d u_c(y)\,\mathrm{d}y = \frac{1}{1+\delta}\left[+\frac{\eta(b)-\eta(y)}{W} + W\delta\left(\tfrac{1}{2}(d^2-b^2) - db + b^2\right) + (d-b)(u_D(b)+\delta u_c(b))\right] \tag{A 18}$$

Equation (A 18) enables the geostrophic equation (2.10) to be integrated to become

$$P_c(d) - P_c(b) = -(d-b)\left\{Wc + \frac{W}{1+\delta}(u_D(b)+\delta u_c(b))\right\} - \frac{1}{1+\delta}\left\{\eta(b)-\eta(y) + W^2\delta\left(\tfrac{1}{2}(d-b)^2\right)\right\}. \tag{A 19}$$

Substituting (2.12) applied at $y = b$ and (2.39), into the Bernoulli function (2.31), yields

$$P_c(b) = -\tfrac{1}{2}u_c^2(b) - \frac{Wb}{\delta}u_c(b) - W^2b^2\frac{1-\delta}{2\delta^2} - Wcb. \tag{A 20}$$

Rearranging the Bernoulli function (A 10) gives

$$P_c(d) = -\tfrac{1}{2}u_c^2(d) - Wcd. \tag{A 21}$$

Evaluating the difference between (A 21) and (A 20) gives

$$P_c(d) - P_c(b) = \tfrac{1}{2}\left(u_c^2(b) - u_c^2(d)\right) + \frac{Wb}{\delta}u_c(b) + W^2b^2\frac{1-\delta}{2\delta^2} + Wc(b-d). \tag{A 22}$$

Equating (A 22) with the previous expression for $P_c(d) - P_c(b)$, (A 19), results in the fourth general equation required to close the problem, which is (2.41) in the main text,

$$\tfrac{1}{2}\left(u_c^2(d)-u_c^2(b)\right) = \frac{(d-b)}{(1+\delta)}(W(u_D(b)+\delta u_c(b))) + \frac{1}{1+\delta}\left(\eta(b)-\eta(d)+\tfrac{1}{2}W^2\delta(d-b)^2\right) + \frac{Wb}{\delta}u_c(b) + W^2b^2\frac{1-\delta}{2\delta^2}. \tag{A 23}$$

A.2. *Momentum equation*

The solution of the momentum equation (2.44) involves the evaluation of a number of integrals:

$$\tfrac{1}{2}c^2 = \int_{A_c}\left(u_c^2 + p_c\right)\mathrm{d}A + \int_{A_a}\left(u_D^2 + p_D\right)\mathrm{d}A + W\int_{V_c} v_c\,\mathrm{d}V + W\int_{V_a} v_D\,\mathrm{d}V.$$

For convenience this is broken down into a number of steps.

Step 1: The terms within the double integrals in (2.44) associated with the current and the ambient fluid are integrated as follows.

Current The velocity term in the first integral becomes

$$\int_{A_c} u_c^2\,\mathrm{d}A = \int_0^d\int_{1-\eta}^1 u_c^2\,\mathrm{d}z\,\mathrm{d}y = \int_0^b u_c^2\,\mathrm{d}y + \int_b^d u_c^2\eta\,\mathrm{d}y. \tag{A 24}$$

The substitution (2.9) is used to replace the pressure term in the first integral and it is integrated to give

$$\int_{A_c} p_c\,\mathrm{d}A = \int_0^d\int_{1-\eta}^1 (P_c + z - 1)\,\mathrm{d}z\,\mathrm{d}y = \int_0^b P_c\,\mathrm{d}y + \int_b^d \left(P_c\eta - \tfrac{1}{2}\eta^2\right)\mathrm{d}y - \tfrac{1}{2}b. \tag{A 25}$$

https://doi.org/10.1017/S0022112004001363 Published online by Cambridge University Press

The third integral, which describes the Coriolis force associated with the across-stream flow within the current, is simplified using the physical argument that since the flow is recirculating and there is no flux into or out of the current, then the volume flux across a vertical plane at y must be equivalent to $Q_c(0;y)$. The substitution (2.29) is also applied, resulting in

$$W\int_{V_c} v_c\,\mathrm{d}V = W\int_0^d Q_c(y)\,\mathrm{d}y = -\delta\int_0^d B(y)\,\mathrm{d}y. \tag{A 26}$$

Ambient fluid The second integral in (2.44) is associated with the downstream ambient fluid. This is integrated with respect to z, then (Part 1: (2.28)), applied downstream, is substituted to give

$$\int_{A_a}\left(u_D^2+p_D\right)\mathrm{d}A = \int_b^1 B_D(y)+\tfrac{1}{2}u_D^2 - Wcy - \eta\left(u_D^2+p_D\right)\mathrm{d}y. \tag{A 27}$$

The fourth integral, which concerns the flow of the ambient fluid around the head of the current, is evaluated using (Part 1: (2.25)), (Part 1: (2.26)) and (Part 1: (2.27)) to give

$$W\int_{V_a} v_D\,\mathrm{d}V = \tfrac{1}{2}Wcb^2 + \int_b^1 (Wcy - B_D(y))\,\mathrm{d}y. \tag{A 28}$$

Adding (A 27) and (A 28) the Bernoulli terms cancel and the expression for the ambient fluid becomes

$$\int_{A_a}\left(u_D^2+p_D\right)\mathrm{d}A + W\int_{V_a} v_D\,\mathrm{d}V = \int_b^d \left(\tfrac{1}{2}u_D^2 - \eta u_D^2 - \eta p_D\right)\mathrm{d}y + \tfrac{1}{2}U_D^2(1-d) + \tfrac{1}{2}Wcb^2. \tag{A 29}$$

Step 2: In the energy-conserving theory for simple flow the velocity of the current equalled zero, therefore the momentum integral consisted of the second and forth integrals in (2.44), plus the integral describing the cross-sectional pressure acting on the current. Hence adding (A 29) to (A 25) gives

$$\int_{A_a}\left(u_D^2+p_D\right)\mathrm{d}A + W\int_{V_a} v_D\,\mathrm{d}V + \int_{A_c} p_c\,\mathrm{d}A = \int_0^b P_c\,\mathrm{d}y + \int_b^d \left(\tfrac{1}{2}u_D^2 - \eta u_D^2 + \tfrac{1}{2}\eta^2\right)\mathrm{d}y + \tfrac{1}{2}U_D^2(1-d) + \tfrac{1}{2}Wcb^2 - \tfrac{1}{2}b. \tag{A 30}$$

Step 3: The sum of the remaining terms in (2.44) for the current equals (A 24) plus (A 26), which gives

$$\int_{A_c} u_c^2\,\mathrm{d}A + W\int_{V_c} v_c\,\mathrm{d}V = \int_0^b u_c^2 - \delta B_c(y)\,\mathrm{d}y + \int_b^d u_c^2\eta - \delta B_c(y)\,\mathrm{d}y. \tag{A 31}$$

The first term in the second integral is integrated by parts using the relationship obtained in the derivation of (2.29)

$$-\frac{\delta}{W}\frac{\mathrm{d}B_c}{\mathrm{d}y} = \eta u_c. \tag{A 32}$$

Then the substitution (2.7) is applied, hence (A 31) becomes

$$\int_{A_c} u_c^2\,\mathrm{d}A + W\int_{V_c} v_c\,\mathrm{d}V = \int_0^b u_c^2 - \delta B_c(y)\,\mathrm{d}y + \int_b^d -\eta B_c(y)\,\mathrm{d}y - \left[\frac{\delta}{W}u_c B_c(y)\right]_b^d. \tag{A 33}$$

https://doi.org/10.1017/S0022112004001363 Published online by Cambridge University Press

Step 4: By combining (A 30) and (A 33) the momentum integral (2.44) becomes

$$\int_0^b \left(P_c + u_c^2 - \delta B_c(y)\right) \mathrm{d}y + \int_b^d \left(\tfrac{1}{2}u_D^2 + \tfrac{1}{2}\eta^2 - \eta B_c(y)\right) \mathrm{d}y - \left[\frac{\delta}{W} u_c B_c(y)\right]_b^d + \tfrac{1}{2}U_D^2(1-d) + \tfrac{1}{2}Wcb^2 - \tfrac{1}{2}b = \tfrac{1}{2}c^2. \quad \text{(A 34)}$$

Step 5: The Bernoulli function (2.26) is used to remove the pressure term in the first integral above. This integral is then solved using two substitutions of (2.7), and (A 32) (noting that $\eta = 1$ where $y \in [0, b]$). Hence, the first integral in (A 34) becomes

$$\int_0^b \left(P_c + u_c^2 - \delta B_c(y)\right) \mathrm{d}y = \frac{\delta}{W}\left[\frac{u_c^3}{6(1-\delta)} - u_c B_c(y)\right]_0^b - \tfrac{1}{2}Wcb^2. \quad \text{(A 35)}$$

The second integral in (A 34) is solved as follows: the substitution (2.13) is applied to the first two terms; (2.8) is used to express the third term as an exact differential; the fourth term is integrated by parts making use of (2.8) and (A 32). Hence the second integral becomes

$$\int_b^d \left(\tfrac{1}{2}u_D^2 + \tfrac{1}{2}\eta^2 - \eta u_D^2 - \eta B_c(y)\right)\mathrm{d}y = \int_b^d \left(\tfrac{1}{2}u_D u_c - \frac{\eta}{\delta}u_D u_c\right) \mathrm{d}y + \frac{1}{W}\left[\tfrac{1}{2}u_D\eta - \tfrac{1}{3}u_D^3 - u_D B_c(y)\right]_b^d. \quad \text{(A 36)}$$

The second term in the remaining integral is simplified further by: substituting a differential for η using (2.7); integrating by parts; substituting the potential vorticity equations (2.8) and (2.7). Hence, the momentum integral (A 34) becomes

$$\int_b^d \tfrac{1}{2}(-u_c(u_D + \delta u_c))\,\mathrm{d}y + \frac{1}{W}\left[\frac{\delta}{6(1-\delta)}u_c^3 - \delta u_c B_c\right]_0^b + \frac{1}{W}\left[\tfrac{1}{6}\delta u_c^3 + \tfrac{1}{2}u_c^2 u_D - \tfrac{1}{3}u_D^2 + \tfrac{1}{2}u_D\eta - \delta u_c B_c(y) - u_D B_c(y)\right]_b^d + \tfrac{1}{2}U_D^2(1-d) - \tfrac{1}{2}b = \tfrac{1}{2}c^2. \quad \text{(A 37)}$$

There does not exist an exact differential, which could be used as a substitution to solve the final integral. However, a solution is possible by substituting the velocity equations (2.25) and (2.26) into the respective terms and integrating directly to give

$$\begin{aligned}
&\int_b^d \tfrac{1}{2}(-u_c(u_D + \delta u_c))\,\mathrm{d}y \\
&= \int_b^d -\tfrac{1}{2}u_c(u_D(0) + \delta u_c(0) + W\delta y)\,\mathrm{d}y \\
&= \big[y((u_c(0)u_D(0))(-(W^2/W'^2)) + \tfrac{1}{2}u_D(0)^2(-(W^2/\delta W'^2)) + \tfrac{1}{2}u_c(0)^2((W^2/W'^2) - \delta)) \\
&\quad + y^2\left(\tfrac{1}{4}(u_c(0))(-W\delta + (W^3/W'^2) - \delta(W^3/W'^2)) + \tfrac{1}{2}u_D(0)(-(W^3/W'^2))\right) \\
&\quad + y^3\left(-\tfrac{1}{6}(W^4/W'^2)\delta\right) + \lambda\left(-\tfrac{1}{2}(W^2/W'^2)\right) + \lambda'\left(\tfrac{1}{2}u_D(0)(W/\delta W'^2) + \tfrac{1}{2}u_c(0)(W/W'^2)\right) \\
&\quad + \tfrac{1}{2}y\lambda'(W^2/W'^2)\big]_b^d,
\end{aligned} \quad \text{(A 38)}$$

where $\lambda = W^{-1}((\eta_0 - (W^2/W'^2))\sinh W'y + (-(W/W')(u_c(0) - u_D(0))\cosh W'y))$ and $\lambda' = \mathrm{d}\lambda/\mathrm{d}y$.

To clarify the momentum equation (A 37), first, the cross-product terms $\frac{1}{2}u_c^2 u_D$ and $u_D B_c(y)$ are replaced using (2.26), (Part 1:(2.28)) and (2.12), to give

$$\tfrac{1}{2}u_c^2 u_D - u_D B_c(y) = \tfrac{1}{2}u_D^3 - u_D B_D(y) - u_D\eta.$$

https://doi.org/10.1017/S0022112004001363 Published online by Cambridge University Press

Secondly, the terms within the brackets are rearranged to refer to either the current or the ambient fluid. Note that for $y \in [0, d]$ $B_c = 0$, according to (2.27). Hence, the general solution to the momentum equation (2.44) becomes

$$\tfrac{1}{2}c^2 = \int_b^d \tfrac{1}{2}(-u_c(u_D + \delta u_c))\,\mathrm{d}y + \frac{1}{W}\left[\frac{\delta^2}{6(1-\delta)}u_c^3\right]_0^b + \left[\frac{\delta}{6W}u_c^3\right]_0^d + \frac{1}{W}\left[\tfrac{1}{6}u_D^3 - \tfrac{1}{2}u_D\eta - u_D B_D(y)\right]_b^d + \tfrac{1}{2}U_D^2(1-d) - \tfrac{1}{2}b \quad \text{(A 39)}$$

where the integral in (A 39) is given by (A 38). Note that, for $y \in [0, b]$, $B_D = 0$ and at $y = d$, $B_D = W(c + (1-d)U_D)$ where (2.32) is substituted into (A 9). The equation (A 39) is the final general equation required to close the problem, which is (2.45) in the main text.

As a check we can show that the general solution for the momentum integral reduces to that for the energy-conserving model with simple flow, by considering the case $u_c = 0$. The assumption of zero velocity for the current will affect the derivation of the ambient fluid pressure and consequently the Bernoulli function $B_D(y)$ in (A 39). Substituting $u_c = 0$ into the geostrophic equation (2.10), the dependent ambient fluid pressure for $y \in [b, d]$ becomes Part 1: (2.16). Therefore, the Bernoulli function applied downstream becomes (for $y \in [b, d]$)

$$B_D = \tfrac{1}{2}u_D^2 - \eta \quad \text{(A 40)}$$

Substituting (A 40) and $u_c = 0$ into (A 39) gives

$$c^2 = \frac{1}{W}\left[-\tfrac{2}{3}u_D^3 + u_D\eta\right]_b^d + U_D^2(1-d) - b. \quad \text{(A 41)}$$

The above expression is equivalent to Part 1: (3.4) without the energy-loss terms (see the discussion of that equation in Part 1).

Appendix B. Governing equations and solutions for each flow geometry

To solve the equations we consider each of the flow geometries in turn, applying the appropriate boundary conditions and obtaining versions of the general equations appropriate to each of the cases. First we give the final equations for each of the cases.

B.1. *Case A*

Case A corresponds to a weak rotation rate, where the current continues to fill the full width of the channel. Thus this case has $b = 0$ and $d = 1$ and the governing equations become:

Momentum equation

$$\tfrac{1}{2}c^2 = \int_0^1 \tfrac{1}{2}(-u_c(u_D + \delta u_c))\,\mathrm{d}y + \frac{\delta}{6W}(u_c(1)^3 - u_c(0)^3) + \frac{1}{W}\left[\tfrac{1}{6}(u_D(1)^3 - u_D(0)^3) + \tfrac{1}{2}(u_D(1)\eta(1) - u_D(0)\eta(0))\right] - u_D(1)c \quad \text{(B 1)}$$

and to evaluate the integral in (B1) it is necessary to substitute the expressions for the flow structure and then integrate (see Appendix A);

Bernoulli equations

$$\eta_0 = \tfrac{1}{2}u_D(0)^2 - \tfrac{1}{2}u_c(0)^2. \quad \text{(B 2)}$$

https://doi.org/10.1017/S0022112004001363 Published online by Cambridge University Press

$$c = \frac{1}{W}\left[\tfrac{1}{2}u_D(1)^2 - \tfrac{1}{2}u_c(1)^2 - \eta(1)\right] \tag{B 3}$$

$$\tfrac{1}{2}\left(u_c^2(1) - u_c^2(0)\right) = \frac{W}{(1+\delta)}(u_D(0) + \delta u_c(0)) + \frac{1}{1+\delta}\left(\eta(0) - \eta(1) + \tfrac{1}{2}W^2\delta\right); \tag{B 4}$$

Flow structure equations

$$\eta(1) = \delta/(1+\delta) + (\eta_0 - \delta/(1+\delta))\cosh W' + (-(W/W')(u_c(0) - u_D(0)))\sinh W, \tag{B 5}$$

$$u_c(1) = u_c(0) - (W^2/\delta W'^2)(u_c(0) - u_D(0)) + W(\delta/(1+\delta)) - (W/\delta W') \times [(\eta_0 - \delta/(1+\delta))\sinh W' + (-(W/W')(u_c(0) - u_D(0)))\cosh W'], \tag{B 6}$$

$$u_D(1) = u_D(0) + (W^2/W'^2)(u_c(0) - u_D(0)) + W(\delta/(1+\delta)) + (W/W')[(\eta_0 - \delta/(1+\delta))\sinh W' + (-(W/W')(u_c(0) - u_D(0)))\cosh W']. \tag{B 7}$$

B.2. *Case B*

Case B corresponds to a moderate rotation rate, where the current banks up against the right-hand wall and outcrops on the surface at $y = d$. Note that there is no shear in the free stream since $\eta(y) = 0$ for $y \in [d, 1]$. The conditions for case B are $b = 0$ and $d < 1$ and the general equations become:

momentum equation

$$\tfrac{1}{2}c^2 = \int_0^d \tfrac{1}{2}(-u_c(u_D + \delta u_c))\,\mathrm{d}y + \frac{\delta}{6W}(u_c(d)^3 - u_c(0)^3) + \frac{1}{W}\left[\tfrac{1}{6}\left(U_D^3 - u_D(0)^3\right) - \tfrac{1}{2}u_D(0)\eta(0) - \tfrac{1}{2}\left(U_D^3 - U_D u_c(d)^2\right)\right] + \tfrac{1}{2}U_D^2(1-d), \tag{B 8}$$

again substituting from the flow structure equations to evaluate the integral;

Bernoulli equations

$$\eta_0 = \tfrac{1}{2}u_D(0)^2 - \tfrac{1}{2}u_c(0)^2, \tag{B 9}$$

$$c = W^1\left[\tfrac{1}{2}U_D^2 - \tfrac{1}{2}u_c(d)^2 + WU_D(d-1)\right], \tag{B 10}$$

$$\tfrac{1}{2}\left(u_c^2(d) - u_c^2(0)\right) = \frac{Wd}{(1+\delta)}(u_D(0) + \delta u_c(0)) + \frac{1}{1+\delta}\left(\eta(0) + \tfrac{1}{2}W^2\delta d^2\right); \tag{B 11}$$

flow structure equations

$$\eta(d) = 0 = \delta/(1+\delta) + (\eta_0 - \delta/(1+\delta))\cosh W'd + (-(W/W')(u_c(0) - u_D(0)))\sinh W'd, \tag{B 12}$$

$$u_c(d) = u_{0c} - (W^2/\delta W'^2)(u_c(0) - u_D(0)) + W(\delta/(1+\delta))\,d - (W/\delta W')[(\eta_0 - \delta/(1+\delta))\sinh W'd + (-(W/W')(u_c(0) - u_D(0)))\cosh W'd], \tag{B 13}$$

$$u_D(d) = U_D = u_{0D} + (W^2/W'^2)(u_c(0) - u_D(0)) + W(\delta/(1+\delta))\,d + (W/W')[(\eta_0 - \delta/(1+\delta))\sinh W'd + (-(W/W')(u_c(0) - u_D(0)))\cosh W'd]. \tag{B 14}$$

B.3. *Case C*

Case C corresponds to a strong rotation rate, where the current has banked up against the right-hand wall to such an extent that it fills the full depth of the channel and

https://doi.org/10.1017/S0022112004001363 Published online by Cambridge University Press

outcrops on the bottom boundary at $y=b$. The conditions for case C are $0<b<d<1$ and the general equations for case C become:

momentum equation

$$\tfrac{1}{2}c^2=\int_b^d \tfrac{1}{2}(-u_c(u_D+\delta u_c))\,\mathrm{d}y+\frac{\delta^2}{W6(1-\delta)}(u_c(b)^3-u_c(0)^3)+\frac{\delta}{6W}(u_c(d)^3-u_c(0)^3)$$
$$+\frac{1}{W}\left[\tfrac{1}{6}\left(U_D^3-u_D(b)^3\right)-\tfrac{1}{2}u_D(b)-\tfrac{1}{2}\left(U_D^3-u_c(d)^2U_D\right)\right]+\tfrac{1}{2}U_D(1-d)-\tfrac{1}{2}b \quad \text{(B 15)}$$

again substituting from the flow structure equations to evaluate the integral;

Bernoulli equations

$$\tfrac{1}{2}u_D^2(b)=\tfrac{1}{2}u_c^2(b)+\frac{Wb}{\delta}u_c(b)+W^2b^2\frac{1-\delta}{2\delta^2}+1, \quad \text{(B 16)}$$

$$c=\frac{1}{W}\left[\tfrac{1}{2}U_D^2-\tfrac{1}{2}u_c(d)^2+WU_D(d-1)\right], \quad \text{(B 17)}$$

$$\tfrac{1}{2}\left(u_c^2(d)-u_c^2(b)\right)=\frac{d-b}{1+\delta}(W(u_D(b)+\delta u_c(b)))+\frac{1}{1+\delta}\left(\eta(b)+\tfrac{1}{2}W^2\delta(d-b)^2\right)$$
$$+\frac{Wb}{\delta}u_c(b)+W^2b^2\frac{1-\delta}{2\delta^2}; \quad \text{(B 18)}$$

flow structure equations

$$u_C(0)=u_C(b)+W[(\delta-1)/\delta](-b), \quad \text{(B 19)}$$

$$u_c(d)=u_C(b)-(W^2/\delta W'^2)(u_c(b)-u_D(b))+W(\delta/(1+\delta))d$$
$$-(W/\delta W')[(\eta_0-\delta/(1+\delta))\sinh W'(d-b)$$
$$+(-(W/W')(u_c(b)-u_D(b)))\cosh W'(d-b)], \quad \text{(B 20)}$$

$$u_D(d)=U_D=u_D(b)+(W^2/W'^2)(u_c(b)-u_D(b))+W(\delta/(1+\delta))d$$
$$+(W/W')[(\eta_0-\delta/(1+\delta))\sinh W'(d-b)$$
$$+(-(W/W')(u_c(b)-u_D(b)))\cosh W'(d-b)], \quad \text{(B 21)}$$

and note $\eta_0=\eta(b)=1$, while $\eta(d)=0$.

B.4. *Case BII*

In evaluating the numerical solutions it became clear that a fourth flow geometry was possible, with the current occupying a substantial part of the channel and the interface intercepting the left-hand wall (looking downstream with respect to the current) and the bottom of the channel. This case was labelled BII, and the conditions for this case are $b>0$ and $d=1$, the general equations for case BII become:

momentum equation

$$\tfrac{1}{2}c^2=\int_b^1 \tfrac{1}{2}(-u_c(u_D+\delta u_c))\,\mathrm{d}y+\frac{\delta^2}{W6(1-\delta)}(u_c(b)^3-u_c(0)^3)+\frac{\delta}{6W}(u_c(1)^3-u_c(0)^3)$$
$$+\frac{1}{W}\left[\tfrac{1}{6}(u_D(1)^3-u_D(b)^3)+\tfrac{1}{2}u_D(1)\eta_D(1)-\tfrac{1}{2}u_D(b)-\tfrac{1}{2}(u_D(1)^3-u_c(1)^2u_D(1))\right]-\tfrac{1}{2}b, \quad \text{(B 22)}$$

https://doi.org/10.1017/S0022112004001363 Published online by Cambridge University Press

again substituting from the flow structure equations to evaluate the integral;

Bernoulli equations

$$\tfrac{1}{2}u_D^2(b) = \tfrac{1}{2}u_c^2(b) + \frac{Wb}{\delta}u_c(b) + W^2b^2\frac{1-\delta}{2\delta^2} + 1, \tag{B 23}$$

$$c = \frac{1}{W}\left[\tfrac{1}{2}u_D(1)^2 - \tfrac{1}{2}u_c(1)^2 - \eta(1)\right], \tag{B 24}$$

$$\tfrac{1}{2}\left(u_c^2(1) - u_c^2(b)\right) = \frac{1-b}{1+\delta}(W(u_D(b) + \delta u_c(b))) + \frac{1}{1+\delta}\left(\eta(b) - \eta(1) + \tfrac{1}{2}W^2\delta(1-b)^2\right) + \frac{Wb}{\delta}u_c(b) + W^2b^2\frac{1-\delta}{2\delta^2}; \tag{B 25}$$

flow structure equations

$$\eta(1) = \delta/(1+\delta) + (\eta(b) - \delta/(1+\delta))\cosh W'(1-b) + (-(W/W')(u_c(b) - u_D(b)))\sinh W'(1-b). \tag{B 26}$$

$u_c(0)$ may be found as in case C using equation (B19), while $u_c(1)$ and $u_D(1)$ may be found as in case C, substituting $d = 1$ in equation (B 20) and (B 21), note also that $\eta_0 = \eta(b) = 1$.

B.5. *Numerical solutions*

While in principle we are solving four equations in four unknowns, in practice the set of equations and unknowns solved for numerically varied between the different cases as follows. For case A, three unknowns were used, the flow speeds in the current and the ambient fluid at the right-hand wall, $u_c(0)$ and $u_D(0)$, and the current speed c. The three equations used were (B 1), (B 3) and (B 4), with $\eta(0)$ substituted into them using (B 2). For case B a fourth unknown, the position of the surface outcropping, d, was added and the equations corresponded to those used for case A: equations (B 8), (B 10) and (B 11) were used, with $\eta(0)$ substituted using equation (B 9). The fourth equation used for case B was the flow structure equation (B 12).

In case C it was more convenient to use five equations in five unknowns. The unknowns were $u_c(b)$, $u_D(b)$, c, b, and d. The five equations were (B 15), (B 16), (B 17) and (B 18), together with an expression for $\eta(d) = 0$ (similar to equation (B 12), but with $(d-b)$ instead of d). For case BII, a similar set of unknowns and equations was used as for case C, except now $d = 1$, leaving the other four unknowns $u_c(b)$, $u_D(b)$, c, and b. The equations were (B 22), (B 23), (B 24) and (B 25).

The simultaneous equations were solved for each case using a Fortran programme and standard NAG routines. In order to get convergence of the numerical scheme an initial guess sufficiently close to the final answer is required. This required some manual intervention and intelligent guesswork, especially for the small δ cases.

REFERENCES

Csanady, G. T. 1971 On the equilibrium shape of the thermocline in a shore zone. *J. Phys. Oceanogr.* **1**, 263–270.

Hacker, J. N. 1996 Gravity currents in rotating channels. PhD thesis, University of Cambridge.

Hacker, J. N. & Linden, P. F. 2002 Gravity currents in rotating channels. Part 1. Steady-state theory. *J. Fluid Mech.* **457**, 295–324.

van Heijst, G. J. F. 1985 Geostrophic adjustment model of tidal mixing front. *J. Phys. Oceanogr.* **15**, 1182–1190.

https://doi.org/10.1017/S0022112004001363 Published online by Cambridge University Press

Hsueh, Y. & Cushman-Roisin, B. 1983 On the formation of surface to bottom fronts over steep topography. *J. Geophys. Res.* **88**, 743–750.

Martin, J. R. & Lane-Serff, G. F. 2004 Rotating gravity currents. Part 1. Energy loss theory. *J. Fluid Mech.* **000**, 000–000.

Moncrieff, M. W. & So, D. W. K. 1989 A hydrodynamical theory of conservative bounded density currents. *J. Fluid Mech.* **198**, 177–197.

Ou, H. W. 1983 Some two-layer models of shelf-slope front: geostrophic adjustment and its maintenance. *J. Phys. Oceanogr.* **13**, 1798–1808.

Stommel, H. & Veronis, G. 1980 Barotrophic response to cooling. *J. Geophys. Res.* **85**, 6661–6666.

https://doi.org/10.1017/S0022112004001363 Published online by Cambridge University Press